Journal of King Saud University – Engineering Sciences (2012) **24**, 1–10

King Saud University

Journal of King Saud University – Engineering Sciences

www.ksu.edu.sa
www.sciencedirect.com

ORIGINAL ARTICLE

Innovative modelling approach for the work piece whirling motion in the lathe machine

Hussien M. Al-Wedyan [a], Mohanad Alata [b,*]

[a] *Al-Balqa'a Applied University, AlHuson University College, Mechanical Engineering Department, Jordan*
[b] *King Saud University, Mechanical Engineering Department, Saudi Arabia*

Received 1 June 2010; accepted 26 November 2010
Available online 22 August 2011

KEYWORDS

Whirling motion;
Modeling;
Turning operation

Abstract An innovative modeling approach to study the whirling motion of the lathe machine in the intermediate turning stage is presented by introducing the system excitation in the form of cutting forces between the cutting edge head and the workpiece. This involves nonhomogeneous boundary conditions with homogeneous equations. The mathematical modeling approach enabled us to solve the problem by modal analysis by transforming the problem into nonhomogeneous equations with homogenous boundary conditions. The proposed approach enables us to predict the whirling motion at different locations on the cutting edge-workpiece system.

1. Introduction

Self-excited vibrations encountered in many machining operations. While the workpiece is under the turning operation, part of the delivered power to the machine is switched to a vibratory power during the machining operation. This creates unrelenting vibrations in the cutting edge-workpiece system. In the lathe machine, the load transmitted through the cutting edge to the workpiece while turning consists of a fluctuating increment of a dynamic origin. The latter initiates from within the complete system of the cutting edge-workpiece system and the nature of the turning process. No investigation has been done on the effect of the workpiece whirling motion on the surface roughness and the geometrical dimensioning and tolerances in the lathe machine. This current study is important in order to look at the causes and some of the phenomena that affect the surface roughness from a different angle. Hence, an innovative approach to find the root cause of this problem will open the doors for researchers to try different ways to suppress this motion, dynamically, and consequently to obtain the best surface finish with minimum irregularities. Al-Wedyan et al. (2007) developed a mathematical approach to study the whirling motion of a boring trepanning association deep hole boring process. They were able to detect the whirling motion of the workpiece-boring bar system at different locations and conducted a number of experiments to validate the theoretical study. The whirling motion of the deep hole boring process were suppressed by using a two electrodynamics shakers in the Y and Z directions in Al-Wedyan et al. (2010). The experimental investigations validated the reduction of the tilted

* Corresponding author.
E-mail address: malata@ksu.edu.sa (M. Alata).

Peer review under responsibility of King Saud University.
doi:10.1016/j.jksues.2011.07.003

Production and hosting by Elsevier

Nomenclature

A_1, A_2	cross section area of the workpiece (m^2)
d_1, d_2	diameter of the workpiece before and after turning (m)
E	Young's modulus (N/m^2)
I_1, I_2	area moment of cross section of the workpiece before and after turning (m^4)
M_1	mass per unit length of the workpiece (kg/m)
M_2	mass per unit length of the workpiece (kg/m)
$Q_1(x,t)$	displacement of the workpiece to the left of the cutting edge (m)
$Q_2(x,t)$	displacement of the boring bar to the right of the cutting edge (m)
γ	weight density of the workpiece (N/m^3)
$\psi(t)$	generalized co-ordinate
ω_n	natural frequency of the system (Hz)

whirl orbit with a close percentage to the theoretical model. Roukema and Altintas (2007) developed a comprehensive exercise in modeling dynamics, kinematics and stability in drilling operations and studied the mechanism of whirling vibrations, which occur due to lateral drill deflections. The mechanism of whirling vibrations is explained, and the hole wall formation during whirling vibrations is investigated by imposing commonly observed whirling motion on the drill. The effect of the drill-hole surface contact during drilling is discussed by observing the discrepancies between the numerical model of the drilling process and experimental measurements. Koak et al. (2009) investigates the whirling, tilting and axial motions of a hard disk drive (HDD) spindle system due to manufacturing errors of fluid dynamic bearings (FDBs). HDD spindle whirls around the sleeve with tilting angle. They showed that the imperfect cylindricity and perpendicularity increase the whirl radius, axial runout and tilting angle of the HDD spindle system. Also, they improved the degradation of dynamic performance due to the imperfect perpendicularity between shaft and thrust plate by allowing the other manufacturing error of the cylindricity of sleeve bore in such a way to compensate the bad effect of the imperfect perpendicularity. Bingwei et al. (2010) addressed the rotordynamic instability of an overhung rotor caused by a hydrodynamic moment due to whirling motion through the structural coupling between whirl and precession modes. The experiments were designed to measure the rotordynamic fluid force moments under various leakage flow rates with various preswirl velocities and various axial clearances between the backshroud and casing. The computation was carried out based on a bulk flow model. It was found that the fluid force moment is generally destabilizing, except for a small region of positive whirling speed ratios. Minis et al. (1990a, 1990 b, > c) studied the vibration in the lathe machine and carried out experiments to validate his findings, which leads to a generalization of the linear stability theory for chatter in turning operations. Cutting conditions affects the Whole characteristics and cause surface errors as Rahman et al. (1988) found using the endrill. It was found that the endrills produced good surface finish and good quality holes under proper cutting parameters (speed, feed and flow rate). The twist drill wondering motion was investigated by Lee et al. (1987) mathematically and experimentally. The model, also, explained the formation of a polygonal hole during initial penetration of drilling. Whirling vibrations were experimentally measured by Fujii et al. (1986a,b) in order to investigate how the whirling vibrations developed in the chisel drill. They used three different chisel drills with different web thicknesses. Fuji et al. (1986) studied the interactions among the effect of drill geometry and drill flank, in starting whirling and developing it, where they find also that the flank surface of the cutting edge is responsible for damping the vibration. Fujii et al. (1988) also investigated the whirling vibrations in a workpiece having a pilot hole, where they find out that whirling motion is a regenerative vibration caused by cutting forces and friction while drilling.

2. Mathematical modeling of the cutting edge-workpiece system

The workpiece end is supported by the tailstock as shown in Fig. 1, where the interaction point between the cutting edge the workpiece is also shown. Continuity conditions are assumed for the deflection, slope, and moment at the interaction point, and shear force increases with the addition of the cutting forces.

The workpiece is a continuous beam clamped at the workpiece driver and a clamped condition is assumed at the tailstock. Hence, we can consider the cutting edge-workpiece system as a multi-span beam and the transverse vibration of this beam in the Y–Z plane has the following governing partial differential equations in the Y and Z directions as

$$EI\frac{\partial^4 Q_y}{\partial X^4}(X,t) + M\frac{\partial^2 Q_y}{\partial t^2}(X,t) = 0 \tag{1}$$

and

$$EI\frac{\partial^4 Q_z}{\partial X^4}(X,t) + M\frac{\partial^2 Q_z}{\partial t^2}(X,t) = 0 \tag{2}$$

where I, M, W_y, W_z, respectively, are

$$I_1, M_1, Q_{1y}, Q_{1z}, \text{ in } \quad 0 < X < L_1$$
$$I_2, M_2, Q_{2y}, Q_{2z}, \text{ in } \quad L_1 < X < L$$
$$M_1 = \frac{\gamma}{g}A_1, \quad M_2 = \frac{\gamma}{g}A_2, \quad I_1 = \frac{\pi}{64}d_1^4,$$
$$I_2 = \frac{\pi}{64}d_2^4, \quad A_1 = \frac{\pi}{4}d_1^2, \quad A_2 = \frac{\pi}{4}d_2^2$$

The boundary conditions in the Y direction are

$$\begin{aligned}
&Q_{1y}(0,t) = 0.0 \quad \text{(a)}, && Q_{1y}(L_1,t) = Q_{2y}(L_1,t) \quad \text{(e)}\\
&Q'_{1y}(0,t) = 0.0 \quad \text{(b)}, && Q'_{1y}(L_1,t) = Q'_{2y}(L_1,t) \quad \text{(f)}\\
&Q_{2y}(L,t) = 0.0 \quad \text{(c)}, && Q''_{1y}(L_1,t) = -Q''_{2y}(L_1,t) \quad \text{(g)}\\
&Q'_{2y}(L,t) = 0.0 \quad \text{(d)}, &&\\
&EI_1 Q'''_{1y}(L_1,t) = -EI_2 Q'''_{2y}(L_1,t) - F_{cy}(t) \quad \text{(h)}
\end{aligned} \tag{3}$$

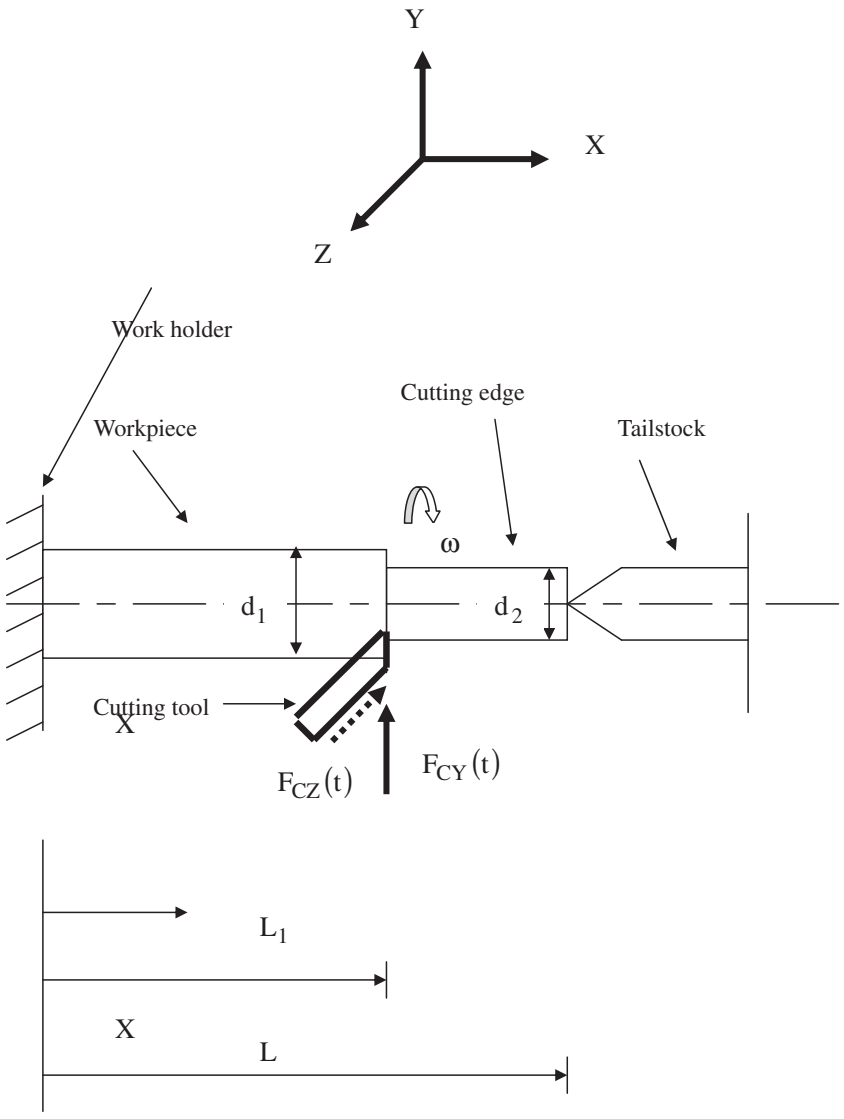

Figure 1 Cutting edge-workpiece system with the cutting forces in the lathe machine.

and the boundary conditions in the Z direction are

$$\begin{aligned}
&Q_{1Z}(0,t) = 0.0 \quad \text{(a)}, \qquad Q_{1Z}(L_1,t) = Q_{2Z}(L_1,t) \quad \text{(e)}\\
&Q'_{1Z}(0,t) = 0.0 \quad \text{(b)}, \qquad Q'_{1Z}(L_1,t) = Q'_{2Z}(L_1,t) \quad \text{(f)}\\
&Q_{2Z}(L,t) = 0.0 \quad \text{(c)}, \qquad Q''_{1Z}(L_1,t) = -Q''_{2Z}(L_1,t) \quad \text{(g)} \qquad (4)\\
&Q'_{2Z}(L,t) = 0.0 \quad \text{(d)},\\
&EI_1 Q'''_{1Z}(L_1,t) = -EI_2 Q'''_{2Z}(L_1,t) - F_{CZ}(t) \quad \text{(h)}
\end{aligned}$$

The nonhomogeneous boundary conditions or time-dependent boundary condition the system is subjected to is given in Eqs. (3h) and (4h). The innovative modeling approach will be used to transform this problem into a problem consisting of nonhomogeneous differential equations with homogeneous boundary conditions which will be solved by modal analysis. So, the solution to this boundary-value problem in both directions is by introducing Eqs. (5) and (6). Given nonhomogeneous boundary condition as in Eqs. (3h) and (4h), which are not vanishing everywhere. Homogeneous boundary conditions usually consist of a relation between the values assumed by the desired function Q and its derivative on the boundary Γ of the domain G in question. We can obtain an equivalent problem with homogeneous boundary conditions by assuming $L[Q] = 0$ is a linear homogeneous equation and the boundary value F can be extended continuously into the interior of G in such a way that $L[F] = g$ is a continuous function in G. Then for the new unknown function $H = Q - F$ we immediately have the differential equation $L[H] = g$ with the homogeneous boundary condition $H = 0$.

$$\begin{aligned}
Q_{1y}(x,t) &= H_{1y}(x,t) + \tau_1(x)F_{cy}(t), \quad 0 < X < L_1\\
Q_{2y}(x,t) &= H_{2y}(x,t) + \tau_2(x)F_{cy}(t), \quad L_1 < X < L
\end{aligned} \qquad (5)$$

$$\begin{aligned}
Q_{1z}(x,t) &= H_{1z}(x,t) + \tau_1(x)F_{cz}(t), \quad 0 < X < L_1\\
Q_{2z}(x,t) &= H_{2z}(x,t) + \tau_2(x)F_{cz}(t), \quad L_1 < X < L
\end{aligned} \qquad (6)$$

The functions $\tau_1(x)$ and $\tau_2(x)$ are chosen to render the boundary conditions for the variables $H_{1y}(x,t)$, $H_{2y}(x,t)$ and $H_{1z}(x,t)$, $H_{2z}(x,t)$ homogeneous.

Several choices for $\tau_1(x)$ and $\tau_2(x)$ are acceptable (Eqs. (9)–(11)). Introducing the boundary conditions of the current problem into Eqs. (5) and (6). Consider Eq. (3h):

$$H'''_{1y}(L_1,t)+kH'''_{2y}(L_1,t)=-F_{cy}(t)\left[k\tau'''_2(L_1)+\tau'''_1(L_1)+\frac{1}{EI_1}\right] \tag{7}$$

For the right hand side of Eq. (7) to be zero:

$$k\tau'''_2(L_1)+\tau'''_1(L_1)+\frac{1}{EI_1}=0 \tag{8}$$

where

$$k=\frac{EI_2}{EI_1}=\frac{I_2}{I_1} \text{ for same } E.$$

Following similar procedure, the boundary conditions from Eq. (3) result in

$$\begin{aligned}
&\tau_1(0)=0 \quad (3a)\\
&\tau'_1(0)=0 \quad (3b)\\
&\tau_2(L)=0 \quad (3c)\\
&\tau'_2(L)=0 \quad (3d)\\
&\tau_2(L_1)-\tau_1(L_1)=0 \quad (3e)\\
&\tau'_2(L_1)-\tau'_1(L_1)=0 \quad (3f)\\
&\tau''_1(L_1)+\tau''_2(L_1)=0 \quad (3g)
\end{aligned} \tag{9}$$

Assuming that

$$\tau'''_1(X)=D_1 \tag{10}$$

Substitute Eq. (10) into Eq. (8), the following equation is obtained:

$$\tau'''_2(X)=-\left(\frac{1}{EI_2}+\frac{D_1}{k}\right) \tag{11}$$

Eqs. (10) and (11) become:

$$\tau_1(X)=\frac{X^3}{6}D_1+\frac{X^2}{2}D_2+XD_3+D_4 \tag{12}$$

$$\tau_2(X)=\frac{-X^3}{6EI_2}-\frac{X^3}{6k}D_1+\frac{X^2}{2}D_5+XD_6+D_7 \tag{13}$$

where the constants D_1, D_2, D_3, D_4, D_5, D_6, D_7 are evaluated by applying the set of boundary conditions in Eq. (9). The values of these constants are presented in Table 1 for $L_1 = 0.5$ m, and $L = 1$ m.

Now introducing Eqs. (5) and (6) in Eq. (1) and (2), respectively, we obtain a set of nonhomogeneous differential equations. In the Y direction:

$$\begin{aligned}
&EI_1H'''_y(x,t)+M_1\ddot{H}_y(x,t)\\
&\quad=-EI_1\tau'''_1(x)F_{cy}(t)-M_1\tau_1(x)\ddot{F}_{cy}(t), \quad 0<X<L_1\\
&EI_2H'''_y(x,t)+M_2\ddot{H}_y(x,t)\\
&\quad=-EI_2\tau'''_2(x)F_{cy}(t)-M_2\tau_2(x)\ddot{F}_{cy}(t), \quad L_1<X<L
\end{aligned} \tag{14}$$

Table 1 Values for the constants of integration for $\tau_1(x)$ and $\tau_2(x)$.

Constant	Value
D_1	3.9245
D_2	−2.8027
D_3	0
D_4	0
D_5	5.6336
D_6	−1.7623
D_7	0.2359

and in Z direction:

$$\begin{aligned}
&EI_1H'''_z(x,t)+M_1\ddot{H}_z(x,t)\\
&\quad=-EI_1\tau'''_1(x)F_{cz}(t)-M_1\tau_1(x)\ddot{F}_{cz}(t), \quad 0<X<L_1\\
&EI_2H'''_z(x,t)+M_2\ddot{H}_z(x,t)\\
&\quad=-EI_2\tau'''_2(x)F_{cz}(t)-M_2\tau_2(x)\ddot{F}_{cz}(t), \quad L_1<X<L
\end{aligned} \tag{15}$$

Now we need to find the natural frequencies with the corresponding eigen functions for the following system of equations:

$$EIH'''_y(x,t)+M\ddot{H}_y(x,t)=0 \tag{16}$$

$$EIH'''_z(x,t)+M\ddot{H}_z(x,t)=0 \tag{17}$$

Under free vibration conditions, we assume:

$$H_y(x,t)=h_y(x)\,e^{i\omega t} \tag{18}$$

$$H_z(x,t)=h_z(x)\,e^{i\omega t} \tag{19}$$

Consider $\overline{X}=\frac{X}{L}$, then $\frac{d}{dX}=\frac{d}{d\overline{X}}\frac{1}{L}$, and accordingly we have

$$h'''_y(\overline{X})-\Theta^4h_y(\overline{X})=0 \tag{20}$$

$$h'''_z(\overline{X})-\Theta^4h_z(\overline{X})=0 \tag{21}$$

where,

$$\Theta^4=\frac{\omega^2M\overline{L}^4}{EI}, \text{ becomes}$$

$$\Theta_1^4=\frac{\omega^2M_1\overline{L}_1^4}{EI_1}, \quad 0<\overline{X}<\overline{L}_1$$

$$\Theta_2^4=\frac{\omega^2M_2\overline{L}^4}{EI_2}, \quad \overline{L}_1<\overline{X}<1$$

$$\overline{L}_1=\frac{L_1}{L}, \quad \overline{L}=\frac{L}{L}=1$$

The solutions in the two regions are

$$\begin{aligned}
&h_{1y}(\bar{x})=A_1\cos\Theta_1\overline{X}+A_2\sin\Theta_1\overline{X}+A_3\cosh\Theta_1\overline{X}\\
&\quad+A_4\sinh\Theta_1\overline{X}, \quad 0<X<\overline{L}_1\\
&h_{2y}(\bar{x})=A_5\cos\Theta_2\overline{X}+A_6\sin\Theta_2\overline{X}+A_7\cosh\Theta_2\overline{X}\\
&\quad+A_8\sinh\Theta_2\overline{X}, \quad \overline{L}_1<X<1
\end{aligned} \tag{22}$$

and in the Z direction:

$$\begin{aligned}
&h_{1z}(\bar{x})=B_1\cos\Theta_1\overline{X}+B_2\sin\Theta_1\overline{X}+B_3\cosh\Theta_1\overline{X}\\
&\quad+B_4\sinh\Theta_1\overline{X}, \quad 0<X<\overline{L}_1\\
&h_{2z}(\bar{x})=B_5\cos\Theta_2\overline{X}+B_6\sin\Theta_2\overline{X}+B_7\cosh\Theta_2\overline{X}\\
&\quad+B_8\sinh\Theta_2\overline{X}, \overline{L}_1<X<1.
\end{aligned} \tag{23}$$

Further

$$\Theta_j^4=\omega^2\frac{M_j\overline{L}_j^4}{(EI)_j}\Rightarrow\omega=\left(\frac{\Theta_j}{\overline{L}_j}\right)^2\sqrt{\frac{(EI)_j}{M_j}}$$

$h_{1y}(\overline{X})$, $h_{2y}(\overline{X})$ in the Y direction and $h_{1z}(\overline{X})$, and $h_{2z}(\overline{X})$ in the Z direction have to satisfy the conditions that their respective fourth derivatives are equal to a constant multiplied by the functions. All the constants A_i and B_i, $i = 1,\ldots,8$ are evaluated using the following boundary conditions in the Y and Z directions:

$$\begin{aligned}
&h_{1y}(0,t)=0.0 \quad (a) && h_{1y}(\overline{L}_1,t)=h_{2y}(\overline{L}_1,t) \quad (e)\\
&h'_{1y}(0,t)=0.0 \quad (b) && h'_{1y}(\overline{L}_1,t)=h'_{2y}(\overline{L}_1,t) \quad (f)\\
&h_{2y}(\overline{L},t)=0.0 \quad (c) && h''_{1y}(\overline{L}_1,t)=-h''_{2y}(\overline{L}_1,t) \quad (g)\\
&h'_{2y}(\overline{L},t)=0.0 \quad (d) && h'''_{1y}(\overline{L}_1,t)=-kh'''_{2y}(\overline{L}_1,t) \quad (h)
\end{aligned} \tag{24}$$

$$\begin{aligned}
&h_{1z}(0,t)=0.0 \quad (a) && h_{1z}(\overline{L}_1,t)=h_{2z}(\overline{L}_1,t) \quad (e)\\
&h'_{1z}(0,t)=0.0 \quad (b) && h'_{1z}(\overline{L}_1,t)=h'_{2z}(\overline{L}_1,t) \quad (f)\\
&h_{2z}(\overline{L},t)=0.0 \quad (c) && h''_{1z}(\overline{L}_1,t)=-h''_{2z}(\overline{L}_1,t) \quad (g)\\
&h'_{2z}(\overline{L},t)=0.0 \quad (d) && h'''_{1z}(\overline{L}_1,t)=-kh'''_{2z}(\overline{L}_1,t) \quad (h)
\end{aligned} \tag{25}$$

From Eqs. (24a) and (24b), it is found that $A_1 = -A_3$ and $A_2 = -A_4$, respectively. The same for Eqs. (25a) and (25b), it is found that $B_1 = -B_3$ and $B_2 = -B_4$, respectively.

These equations are written in the form:

$$[G]_{6X6}\{A\}_{6X1} = \{0\} \quad \text{and} \quad [H]_{6X6}\{B\}_{6X1} = \{0\} \tag{26}$$

For a nontrivial solutions $|G| = 0, |H| = 0$. Any one will give the characteristic equation, where $|G|$ and $|H|$ are the determinant of the coefficient matrices [G] and [H], respectively. Plotting the frequency equation against $\sqrt{\omega_n}$ yields the roots of the frequency equation for the first eight natural frequencies of the Cutting edge-Workpiece system. Table 2 presents the first eight natural frequencies. The frequency equation is

$$\begin{aligned}
|H| = {} & 8 + 4\cos\left(\sqrt{\omega_n}\left(-\Theta_2\overline{L}_1 + \Theta_1\overline{L}_1 + \Theta_2\right)\right)\\
& \times \cosh\left(\sqrt{\omega_n}\left(-\Theta_2\overline{L}_1 + \Theta_1\overline{L}_1 + \Theta_2\right)\right) - 4\\
& \times \cos\left(\sqrt{\omega_n}\left(-\Theta_2\overline{L}_1 + \Theta_1\overline{L}_1 + \Theta_2\right)\right)\\
& \times \cosh\left(\sqrt{\omega_n}\left(-\Theta_2\overline{L}_1 - \Theta_1\overline{L}_1 + \Theta_2\right)\right) - 4\\
& \times \cos\left(\sqrt{\omega_n}\left(-\Theta_2\overline{L}_1 - \Theta_1\overline{L}_1 + \Theta_2\right)\right)\\
& \times \cosh\left(\sqrt{\omega_n}\left(-\Theta_2\overline{L}_1 + \Theta_1\overline{L}_1 + \Theta_2\right)\right) - 4\\
& \times \cos\left(\sqrt{\omega_n}\left(-\Theta_2\overline{L}_1 - \Theta_1\overline{L}_1 + \Theta_2\right)\right)\\
& \times \cosh\left(\sqrt{\omega_n}\left(-\Theta_2\overline{L}_1 - \Theta_1\overline{L}_1 + \Theta_2\right)\right)
\end{aligned}$$

The normal modes corresponding to these natural frequencies are

Table 2 Presents the first eight natural frequencies.

Natural frequency number	ω_n (Hz)
1	24
2	242.2
3	573.24
4	1019.1
5	1592.36
6	2293
7	3121.02
8	4076

$$\begin{aligned}
h_{1yi}(\bar{x}) &= \overline{A}_3\left(\cosh\Theta_{1i}\overline{X} - \cos\Theta_{1i}\overline{X}\right) - \overline{A}_4\left(\sinh\Theta_{1i}\overline{X} - \sin\Theta_{1i}\overline{X}\right)\\
h_{2yi}(\bar{x}) &= \overline{A}_5\cos\Theta_{2i}\overline{X} + \overline{A}_6\sin\Theta_{2i}\overline{X} + \overline{A}_7\cosh\Theta_{2i}\overline{X} + \overline{A}_8\sinh\Theta_{2i}\overline{X}
\end{aligned} \tag{27}$$

$$\begin{aligned}
h_{1zi}(\bar{x}) &= \overline{B}_3\left(\cosh\Theta_{1i}\overline{X} - \cos\Theta_{1i}\overline{X}\right) - \overline{B}_4\left(\sinh\Theta_{1i}\overline{X} - \sin\Theta_{1i}\overline{X}\right)\\
h_{2zi}(\bar{x}) &= \overline{B}_5\cos\Theta_{2i}\overline{X} + \overline{B}_6\sin\Theta_{2i}\overline{X} + \overline{B}_7\cosh\Theta_{2i}\overline{X} + \overline{B}_8\sinh\Theta_{2i}\overline{X}
\end{aligned} \tag{28}$$

$$\Theta_{1i}^4 = \omega^4\frac{M_2\overline{L}_2^4}{(EI)_2}\alpha_1\lambda_1 k, \quad \Theta_{2i}^4 == \Theta_{2i}^4 = \omega^2\frac{M_2\overline{L}^4}{(EI)_2}\frac{1}{\alpha_1\lambda_1 k},$$

where

$$\frac{1}{k} = \frac{(EI)_1}{(EI)_2}, \quad \alpha_1 = \frac{M_1}{M_2}, \quad \lambda_1 = \frac{\overline{L}_1^4}{\overline{L}^4}$$

The values for $\overline{A}_i$ and $\overline{B}_i$, $i = 3, 5, \ldots, 8$ are presented in Table 3.

Now, in order to solve the nonhomogeneous differential Eqs. (14) and (15), assume the solution in terms of normal modes:

$$\begin{aligned}
h_y(\bar{x},t) &= \sum_{n=1}^{\infty} h_{yn}(\bar{x})\psi_{yn}(t)\\
h_z(\bar{x},t) &= \sum_{n=1}^{\infty} h_{zn}(\bar{x})\psi_{zn}(t)
\end{aligned} \tag{29}$$

Introducing Eq. (29) into Eq. (14) in the Y direction we obtain:

$$\begin{aligned}
&\sum_{n=1}^{\infty}\left(\psi_{yn}(t)h''''_{yn}(\bar{x}) + \ddot{\psi}_{yn}(t)\frac{M_1}{EI_1}h_{yn}(\bar{x})\right)\\
&\quad = -\tau''''_1(\bar{x})F_{cy}(t) - \frac{M_1}{EI_1}\tau_1(\bar{x})\ddot{F}_{cy}(t), \quad 0 < \overline{X} < \overline{L}_1\\
&\sum_{n=1}^{\infty}\left(\psi_{yn}(t)h''''_{yn}(\bar{x}) + \ddot{\psi}_{yn}(t)\frac{M_2}{EI_2}h_{yn}(\bar{x})\right)\\
&\quad = -\tau''''_2(\bar{x})F_{cy}(t) - \frac{M_2}{EI_2}\tau_2(\bar{x})\ddot{F}_{cy}(t), \quad \overline{L}_1 < \overline{X} < 1
\end{aligned} \tag{30}$$

and introduce Eq. (30) into Eq. (15) in the Z direction, we obtain:

$$\begin{aligned}
&\sum_{n=1}^{\infty}\left(\psi_{zn}(t)h''''_{zn}(\bar{x}) + \ddot{\psi}_{zn}(t)\frac{M_1}{EI_1}h_{zn}(\bar{x})\right)\\
&\quad = -\tau''''_1(\bar{x})F_{cz}(t) - \frac{M_1}{EI_1}\tau_1(\bar{x})\ddot{F}_{cz}(t), \quad 0 < \overline{X} < \overline{L}_1\\
&\sum_{n=1}^{\infty}\left(\psi_{zn}(t)h''''_{zn}(\bar{x}) + \ddot{\psi}_{zn}(t)\frac{M_2}{EI_2}h_{zn}(\bar{x})\right)\\
&\quad = -\tau''''_2(\bar{x})F_{cz}(t) - \frac{M_2}{EI_2}\tau_2(\bar{x})\ddot{F}_{cz}(t), \quad \overline{L}_1 < \overline{X} < 1
\end{aligned} \tag{31}$$

and since $h_{1yn}(\bar{x})$, $h_{2yn}(\bar{x})$ and $h_{1zn}(\bar{x})$, $h_{2zn}(\bar{x})$ and ωn satisfies Eqs. (20) and (21), Eqs. (30) and (31) can be written as, first in the Y direction:

Table 3 The arbitrary constants for the normal modes at the first five natural frequencies.

	ω_1	ω_2	ω_3	ω_4	ω_5
$\overline{A}_4, \overline{B}_4$	−0.5561	0.4565	−0.0981	−0.27308	−0.98528
$\overline{A}_5, \overline{B}_5$	−0.1180	2.5563	−3.3823	−4.2784	−6.1784
$\overline{A}_6, \overline{B}_6$	0.8707	2.5674	−2.2613	6.25506	−0.7482
$\overline{A}_7, \overline{B}_7$	−5.5677	−373.847	−0.0001	1317192	1911.026
$\overline{A}_8, \overline{B}_8$	5.5931	373.847	0.0001	−1317192	−1911.025

$$\begin{aligned}
&\sum_{n=1}^{\infty}\left(\left(\ddot{\psi}_{yn}(t)+\omega_n^2\psi_{yn}(t)\right)\frac{M_1}{EI_1}h_{yn}(\bar{x})\right)\\
&\quad=-\left[\tau_1''''(\bar{x})F_{cy}(t)+\frac{M_1}{EI_1}\tau_1(\bar{x})\ddot{F}_{cy}(t)\right],\quad 0<\overline{X}<\overline{L}_1\\
&\sum_{n=1}^{\infty}\left(\left(\ddot{\psi}_{yn}(t)+\omega_n^2\psi_{yn}(t)\right)\frac{M_2}{EI_2}h_{yn}(\bar{x})\right)\\
&\quad=-\left[\tau_2''''(\bar{x})F_{cy}(t)+\frac{M_2}{EI_2}\tau_2(\bar{x})\ddot{F}_{cy}(t)\right],\quad \overline{L}_1<\overline{X}<1
\end{aligned}\tag{32}$$

and in the Z direction:

$$\begin{aligned}
&\sum_{n=1}^{\infty}\left(\left(\ddot{\psi}_{zn}(t)+\omega_n^2\psi_{zn}(t)\right)\frac{M_1}{EI_1}h_{zn}(\bar{x})\right)\\
&\quad=-\left[\tau_1''''(\bar{x})F_{cz}(t)+\frac{M_1}{EI_1}\tau_1(\bar{x})\ddot{F}_{cz}(t)\right],\quad 0<\overline{X}<\overline{L}_1\\
&\sum_{n=1}^{\infty}\left(\left(\ddot{\psi}_{zn}(t)+\omega_n^2\psi_{zn}(t)\right)\frac{M_2}{EI_2}h_{zn}(\bar{x})\right)\\
&\quad=-\left[\tau_2''''(\bar{x})F_{cz}(t)+\frac{M_2}{EI_2}\tau_2(\bar{x})\ddot{F}_{cz}(t)\right],\quad \overline{L}_1<\overline{X}<1
\end{aligned}\tag{33}$$

To find the solution in the three regions, we have to uncouple these equations using the orthogonal property of the Eigen function and integrate with respect to $\overline{X}$ over the domain. The orthogonal properties are as follows:

$$\begin{aligned}
&\int_0^{\overline{L}_1}h_{1yn}(\bar{x})h_{1ym}(\bar{x})\,\mathrm{d}\bar{x}+\int_{\overline{L}_1}^{1}h_{2yn}(\bar{x})h_{2ym}(\bar{x})\,\mathrm{d}\bar{x}=\delta_{nm},\quad \text{if } m=n\\
&\int_0^{\overline{L}_1}h_{1yn}(\bar{x})h_{1ym}(\bar{x})\,\mathrm{d}\bar{x}+\int_{\overline{L}_1}^{1}h_{2yn}(\bar{x})h_{2ym}(\bar{x})\,\mathrm{d}\bar{x}=0,\quad \text{if } m\neq n\\
&\int_0^{\overline{L}_1}h_{1zn}(\bar{x})h_{1zm}(\bar{x})\,\mathrm{d}\bar{x}+\int_{\overline{L}_1}^{1}h_{2zn}(\bar{x})h_{2zm}(\bar{x})\,\mathrm{d}\bar{x}=\delta_{nm},\quad \text{if } m=n\\
&\int_0^{\overline{L}_1}h_{1zn}(\bar{x})h_{1zm}(\bar{x})\,\mathrm{d}\bar{x}+\int_{\overline{L}_1}^{1}h_{2zn}(\bar{x})h_{2zm}(\bar{x})\,\mathrm{d}\bar{x}=0,\quad \text{if } m\neq n
\end{aligned}$$

Hence, we obtain an infinite set of uncoupled ordinary differential equations in Y and Z directions for the two regions of the beam:

$$\begin{aligned}
&\ddot{\psi}_{yi}(t)+2\xi\Theta_{1i}^2\dot{\psi}_{yi}(t)+\Theta_{1i}^4\psi_{yi}(t)=\vartheta_{yi}(t)\\
&\ddot{\psi}_{yi}(t)+2\xi\Theta_{2i}^2\dot{\psi}_{yi}(t)+\Theta_{2i}^4\psi_{yi}(t)=\vartheta_{yi}(t)
\end{aligned}\tag{34}$$

Similarly in Z direction:

$$\begin{aligned}
&\ddot{\psi}_{zi}(t)+2\xi\Theta_{1i}^2\dot{\psi}_{zi}(t)+\Theta_{1i}^4\psi_{zi}(t)=\vartheta_{zi}(t)\\
&\ddot{\psi}_{zi}(t)+2\xi\Theta_{2i}^2\dot{\psi}_{zi}(t)+\Theta_{2i}^4\psi_{zi}(t)=\vartheta_{zi}(t)
\end{aligned}\tag{35}$$

where

$$\begin{aligned}
\vartheta_{yi}(t)&=F_y(t)\left[\int_0^{\overline{L}_1}h_{1yi}(\bar{x})\,\mathrm{d}\bar{x}+\int_{\overline{L}_1}^{1}h_{2yi}(\bar{x})\,\mathrm{d}\bar{x}\right]\\
\vartheta_{zi}(t)&=F_z(t)\left[\int_0^{\overline{L}_1}h_{1zi}(\bar{x})\,\mathrm{d}\bar{x}+\int_{\overline{L}_1}^{1}h_{2zi}(\bar{x})\,\mathrm{d}\bar{x}\right]\\
F_y(t)&=-\left[\phi_{1yi}^*F_{cy}(t)+\phi_{1yi}\ddot{F}_{cy}(t)\right]\quad\text{and}\\
&\qquad I=I_1,\ \ M=M_1,\quad 0<\overline{X}<\overline{L}_1\\
&=-\left[\phi_{2yi}^*F_{cy}(t)+\phi_{2yi}\ddot{F}_{cy}(t)\right]\quad\text{and}\\
&\qquad I=I_2,\ \ M=M_2,\quad \overline{L}_1<\overline{X}<1
\end{aligned}$$

$$\begin{aligned}
F_y(t)&=-\left[\phi_{1zi}^*F_{cz}(t)+\phi_{1zi}\ddot{F}_{cz}(t)\right]\quad\text{and}\\
&\qquad I=I_1,\ \ M=M_1,\quad 0<\overline{X}<\overline{L}_1\\
&=-\left[\phi_{2zi}^*F_{cz}(t)+\phi_{2zi}\ddot{F}_{cz}(t)\right]\quad\text{and}\\
&\qquad I=I_2,\ \ M=M_2,\quad \overline{L}_1<\overline{X}<1
\end{aligned}$$

where

$$\begin{aligned}
&\phi_{1yi}^*=\int_0^{\overline{L}_1}h_{1yi}(\bar{x})\tau_1''''(\bar{x})\,\mathrm{d}\bar{x},\qquad \phi_{1yi}=\int_0^{\overline{L}_1}h_{1yi}(\bar{x})\frac{M_1}{EI_1}\tau_1(\bar{x})\,\mathrm{d}\bar{x},\\
&\phi_{2yi}^*=\int_{\overline{L}_1}^{1}h_{2yi}(\bar{x})\tau_2''''(\bar{x})\,\mathrm{d}\bar{x},\qquad \phi_{2yi}=\int_{\overline{L}_1}^{1}h_{2yi}(\bar{x})\frac{M_2}{EI_2}\tau_2(\bar{x})\,\mathrm{d}\bar{x},\\
&\phi_{1zi}^*=\int_0^{\overline{L}_1}h_{1zi}(\bar{x})\tau_1''''(\bar{x})\,\mathrm{d}\bar{x},\qquad \phi_{1zi}=\int_0^{\overline{L}_1}h_{1zi}(\bar{x})\frac{M_1}{EI_1}\tau_1(\bar{x})\,\mathrm{d}\bar{x},\\
&\phi_{2zi}^*=\int_{\overline{L}_1}^{1}h_{2zi}(\bar{x})\tau_2''''(\bar{x})\,\mathrm{d}\bar{x},\qquad \phi_{2zi}=\int_{\overline{L}_1}^{1}h_{2zi}(\bar{x})\frac{M_2}{EI_2}\tau_2(\bar{x})\,\mathrm{d}\bar{x},
\end{aligned}$$

The whirling motions at different sections of the cutting edge-workpiece system are plotted at speed of 100 rad/s and with cutting forces in the form of

$$\begin{aligned}
F_{cy}(t)&=F_{c0}\cos(\omega_t)\\
F_{cz}(t)&=F_{c0}\sin(\omega_t)
\end{aligned}$$

The solution for the set of equations in Y direction (Eqs. (34) and (35)) are obtained by the convolution integral or superposition integral. It is based on the superposition of the responses of the system to a sequence of impulses. Let the variable of integration be (τ) between the limits of integration (0) and (t) and the elemental impulse is $N_n(\tau)d\tau$. So the complete solution for these equations with zero initial conditions is

$$\begin{aligned}
\psi_{yi}(t)&=\left(\frac{1}{\omega_i}\int_0^t\vartheta_{yi}(\tau)\,\mathrm{e}^{-\xi w_i(t-\tau)}\sin\omega_i(t-\tau)\,\mathrm{d}\tau\right)\\
\psi_{zi}(t)&=\left(\frac{1}{\omega_i}\int_0^t\vartheta_{zi}(\tau)\,\mathrm{e}^{-\xi w_i(t-\tau)}\sin\omega_i(t-\tau)\,\mathrm{d}\tau\right)
\end{aligned}\tag{36}$$

The complete solution for the current problem is as follows:

$$\begin{aligned}
Q_{1y}(\bar{x},t)&=\sum_{i=1}^{\infty}h_{1yi}(\bar{x})\left(\frac{1}{\omega_i}\int_0^t\vartheta_{yi}(\tau)\,\mathrm{e}^{-\xi w_i(t-\tau)}\sin\omega_i(t-\tau)\,\mathrm{d}\tau\right)\\
&\quad+\tau_1(\bar{x})F_{cy}(t)\\
&\text{in the region } 0<\overline{X}<\overline{L}_1,\\
Q_{2y}(\bar{x},t)&=\sum_{n=1}^{\infty}h_{2yi}(\bar{x})\left(\frac{1}{\omega_i}\int_0^t\vartheta_{yi}(\tau)\,\mathrm{e}^{-\xi w_i(t-\tau)}\sin\omega_i(t-\tau)\,\mathrm{d}\tau\right)\\
&\quad+\tau_2(\bar{x})F_{cy}(t)\\
&\text{in the region } \overline{L}_1<\overline{X}<1,
\end{aligned}\tag{37}$$

and in the Z direction

$$\begin{aligned}
Q_{1z}(\bar{x},t)&=\sum_{i=1}^{\infty}h_{1zi}(\bar{x})\left(\frac{1}{\omega_i}\int_0^t\vartheta_{zi}(\tau)\,\mathrm{e}^{-\xi w_i(t-\tau)}\sin\omega_i(t-\tau)\,\mathrm{d}\tau\right)\\
&\quad+\tau_1(\bar{x})F_{cz}(t)\ \text{in the region } 0<\overline{X}<\overline{L}_1,\\
Q_{2z}(\bar{x},t)&=\sum_{n=1}^{\infty}h_{2zi}(\bar{x})\left(\frac{1}{\omega_i}\int_0^t\vartheta_{zi}(\tau)\,\mathrm{e}^{-\xi w_i(t-\tau)}\sin\omega_i(t-\tau)\,\mathrm{d}\tau\right)\\
&\quad+\tau_2(\bar{x})F_{cz}(t)\ \text{in the region } \overline{L}_1<\overline{X}<1.
\end{aligned}\tag{38}$$

Substituting the forces in the solution in the Y directions:

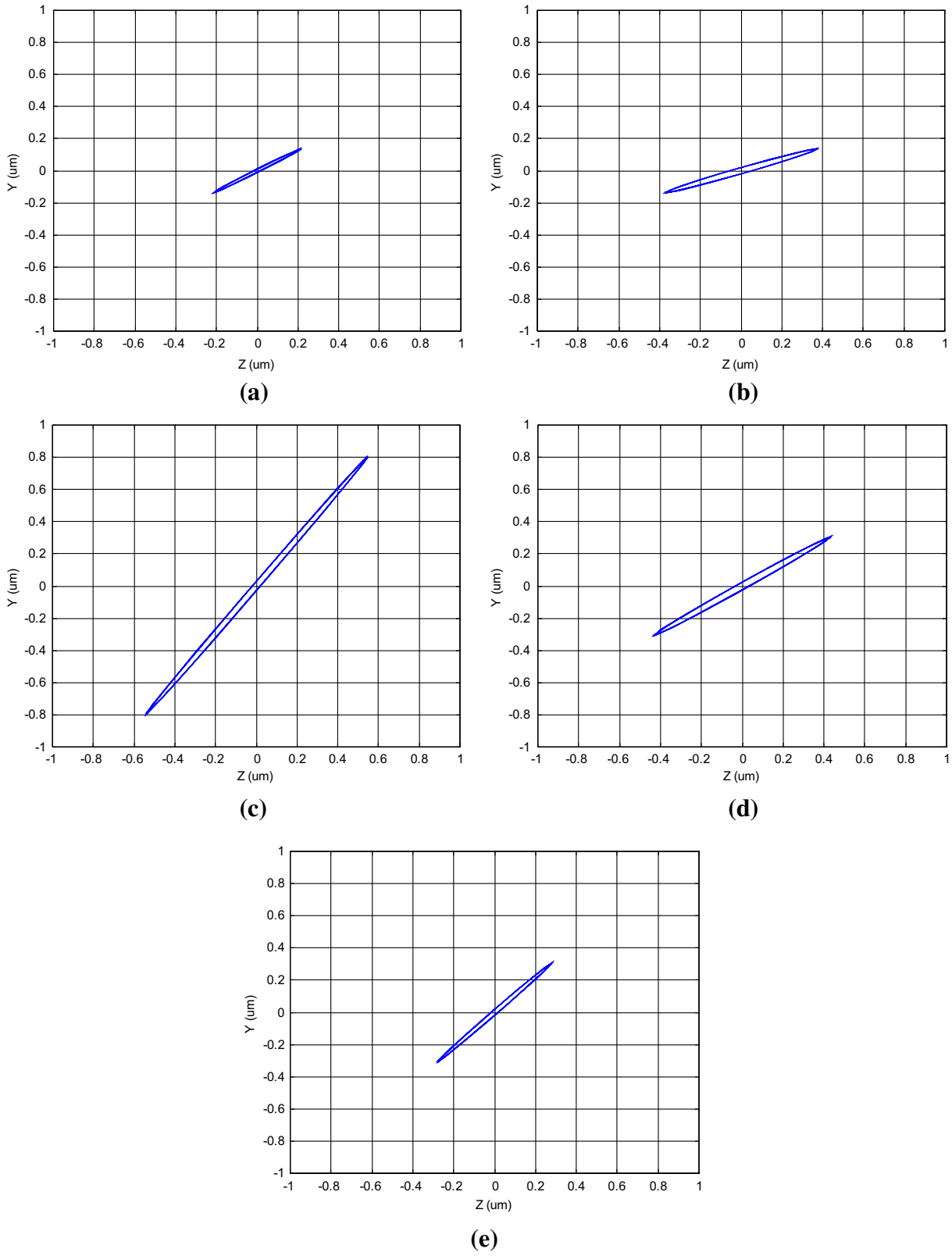

Figure 2 Whirling motion of the cutting edge-workpiece system for the lathe machine at (a) $\overline{X} = 0.1$, (b) $\overline{X} = 0.3$, (c) $\overline{X} = 0.5$, (d) $\overline{X} = 0.7$, and (e) $\overline{X} = 0.9$.

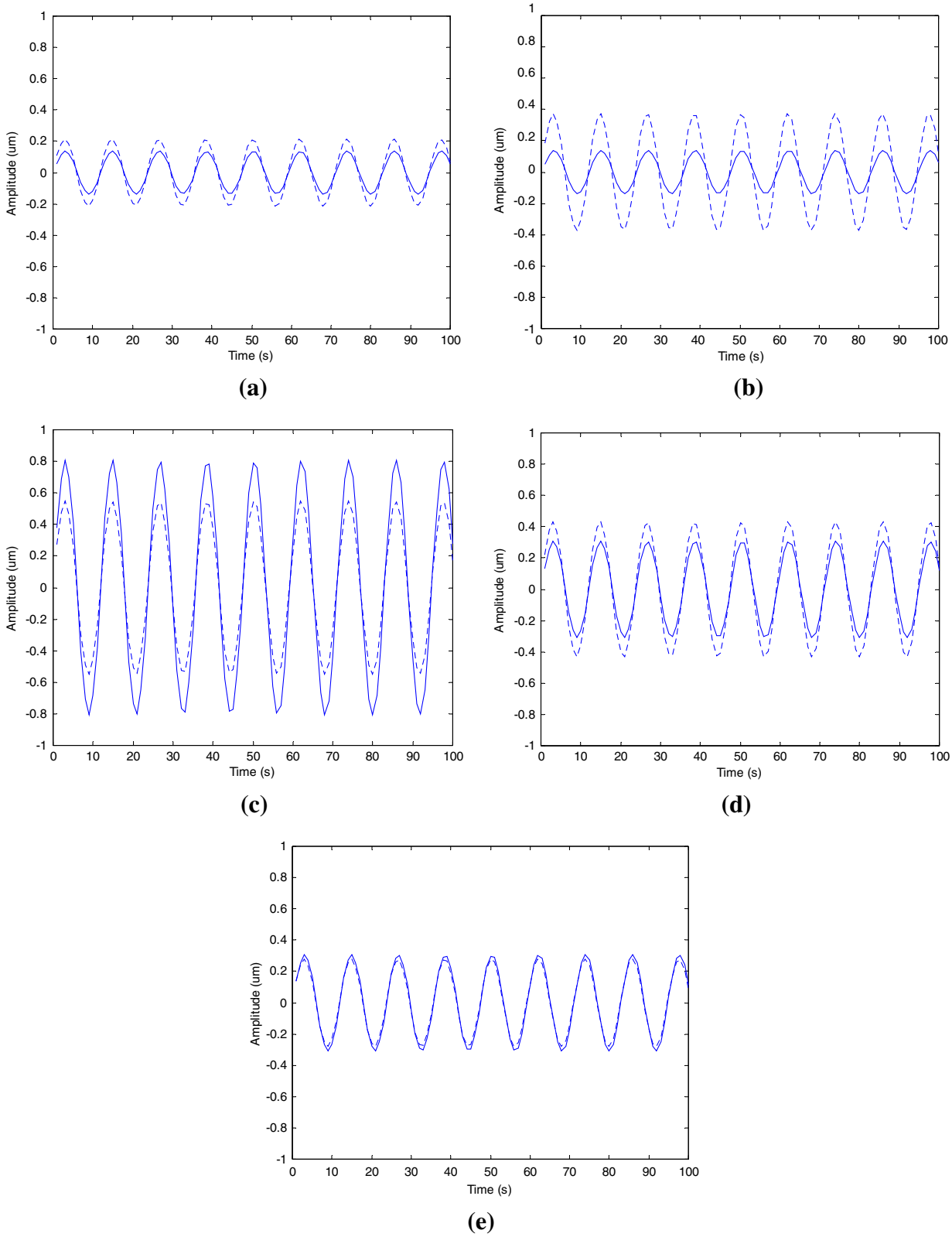

Figure 3 Displacement in the Y (---) and Z (___) directions for the workpiece at (a) $\overline{X} = 0.1$, (b) $\overline{X} = 0.3$, (c) $\overline{X} = 0.5$, (d) $\overline{X} = 0.7$, and (e) $\overline{X} = 0.9$.

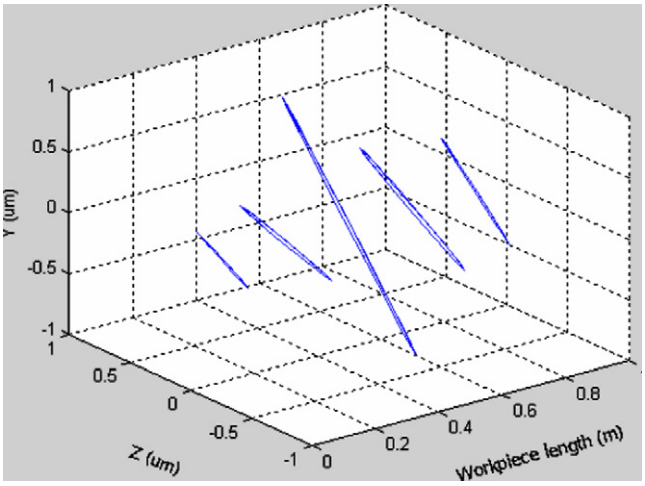

Figure 4 One figure plot of the whirling motion at different location of the workpiece.

Table 4 Whirl diameters for Fig. 2 at different locations on the workpiece.

Fig. 3	Whirl diameter (μm)
(a)	0.4
(b)	0.75
(c)	0.96
(d)	0.82
(e)	0.48

$$
\begin{aligned}
Q_{1y}(\bar{x},t) &= \sum_{i=1}^{\infty} h_{y1i}(\bar{x}) \\
&\times \left(\frac{1}{\omega_i} \int_0^t \begin{pmatrix} -\left[\phi^*_{1yi} F_{cy}(\tau) + \phi_{1yi} \ddot{F}_{cy}(\tau)\right] \\ -\left[\phi^*_{2yi} F_{cy}(\tau) + \phi_{2yi} \ddot{F}_{cy}(\tau)\right] \end{pmatrix} \mathrm{e}^{-\xi w_i (t-\tau)} \sin \omega_i (t-\tau)\, \mathrm{d}\tau \right) \\
&+ \tau_1(\bar{x}) F_{cy}(t) \text{ in the range of } 0 < \overline{X} < \overline{L}_1 \\
Q_{2y}(\bar{x},t) &= \sum_{i=1}^{\infty} h_{y2i}(\bar{x}) \\
&\times \left(\frac{1}{\omega_i} \int_0^t \begin{pmatrix} -\left[\phi^*_{1yi} F_{cy}(\tau) + \phi_{1yi} \ddot{F}_{cy}(\tau)\right] \\ -\left[\phi^*_{2yi} F_{cy}(\tau) + \phi_{2yi} \ddot{F}_{cy}(\tau)\right] \end{pmatrix} \mathrm{e}^{-\xi w_i (t-\tau)} \sin \omega_i (t-\tau)\, \mathrm{d}\tau \right) \\
&+ \tau_2(\bar{x}) F_{cy}(t) \text{ in the range of } \overline{L}_1 < \overline{X} < 1
\end{aligned} \tag{39}
$$

and the solution in the Z direction will be

$$
\begin{aligned}
Q_{1z}(\bar{x},t) &= \sum_{i=1}^{\infty} h_{z1i}(\bar{x}) \\
&\times \left(\frac{1}{\omega_i} \int_0^t \begin{pmatrix} -\left[\phi^*_{1zi} F_{cz}(\tau) + \phi_{1zi} \ddot{F}_{cz}(\tau)\right] \\ -\left[\phi^*_{2zi} F_{cz}(\tau) + \phi_{2zi} \ddot{F}_{cz}(\tau)\right] \end{pmatrix} \mathrm{e}^{-\xi w_i (t-\tau)} \sin \omega_i (t-\tau)\, \mathrm{d}\tau \right) \\
&+ \tau_1(\bar{x}) F_{cz}(t) \text{ in the range of } 0 < \overline{X} < \overline{L}_1 \\
Q_{2z}(\bar{x},t) &= \sum_{i=1}^{\infty} h_{z2i}(\bar{x}) \\
&\times \left(\frac{1}{\omega_i} \int_0^t \begin{pmatrix} -\left[\phi^*_{1zi} F_{cz}(\tau) + \phi_{1zi} \ddot{F}_{cz}(\tau)\right] \\ -\left[\phi^*_{2zi} F_{cz}(\tau) + \phi_{2zi} \ddot{F}_{cz}(\tau)\right] \end{pmatrix} \mathrm{e}^{-\xi w_i (t-\tau)} \sin \omega_i (t-\tau)\, \mathrm{d}\tau \right) \\
&+ \tau_2(\bar{x}) F_{cz}(t) \text{ in the range of } \overline{L}_1 < \overline{X} < 1
\end{aligned} \tag{40}
$$

but $\phi^*_{1yi} = \phi^*_{2yi} = 0$ in the Y direction and $\phi^*_{1zi} = \phi^*_{1zi} = 0$ in the Z direction. This simplifies the final solution to

$$
\begin{aligned}
Q_{1y}(\bar{x},t) &= \sum_{i=1}^{\infty} h_{y1i}(\bar{x}) \\
&\times \left(\frac{1}{\omega_i} \int_0^t -\left(\phi_{1yi} \ddot{F}_{cy}(\tau) + \phi_{2yi} \ddot{F}_{cy}(\tau)\right) \mathrm{e}^{-\xi w_i (t-\tau)} \sin \omega_i (t-\tau)\, \mathrm{d}\tau \right) \\
&+ \tau_1(\bar{x}) F_{cy}(t) \text{ in the range of } 0 < \overline{X} < \overline{L}_1 \\
Q_{2y}(\bar{x},t) &= \sum_{i=1}^{\infty} h_{y2i}(\bar{x}) \\
&\times \left(\frac{1}{\omega_i} \int_0^t -\left(\phi_{1yi} \ddot{F}_{cy}(\tau) + \phi_{2yi} \ddot{F}_{cy}(\tau)\right) \mathrm{e}^{-\xi w_i (t-\tau)} \sin \omega_i (t-\tau)\, \mathrm{d}\tau \right) \\
&+ \tau_2(\bar{x}) F_{cy}(t) \text{ in the range of } \overline{L}_1 < \overline{X} < 1
\end{aligned} \tag{41}
$$

and the solution in the Z direction will be:

$$
\begin{aligned}
Q_{1z}(\bar{x},t) &= \sum_{i=1}^{\infty} h_{z1i}(\bar{x}) \\
&\times \left(\frac{1}{\omega_i} \int_0^t -\left(\phi_{1zi} \ddot{F}_{cz}(\tau) + \phi_{2zi} \ddot{F}_{cz}(\tau)\right) \mathrm{e}^{-\xi w_i (t-\tau)} \sin \omega_i (t-\tau)\, \mathrm{d}\tau \right) \\
&+ \tau_1(\bar{x}) F_{cz}(t) \text{ in the range of } 0 < \overline{X} < \overline{L}_1 \\
Q_{2z}(\bar{x},t) &= \sum_{i=1}^{\infty} h_{z2i}(\bar{x}) \\
&\times \left(\frac{1}{\omega_i} \int_0^t -\left(\phi_{1zi} \ddot{F}_{cz}(\tau) + \phi_{2zi} \ddot{F}_{cz}(\tau)\right) \mathrm{e}^{-\xi w_i (t-\tau)} \sin \omega_i (t-\tau)\, \mathrm{d}\tau \right) \\
&+ \tau_2(\bar{x}) F_{cz}(t) \text{ in the range of } \overline{L}_1 < \overline{X} < 1
\end{aligned} \tag{42}
$$

in the Y direction $\phi_{1yi} F_{c_o y} = \phi_{2yi} F_{c_o y} = \text{constant}$, and the same in the Z direction $\phi_{1zi} F_{c_o z} = \phi_{2zi} F_{c_o z} = \text{constant}$.

So, in order to arrive at the final solution, the integrals in Appendix A are used. It is seen from those integrals that the final solution will have a transient (which will die out after a while) and steady state solution. The steady state solution for the self-excited motion at $\omega = 100$ rad/s which is below the first natural frequency, is plotted for AISI 1020 steel with $E = 200$ GPa, and $\gamma = 77177.98$ N/m^3 in Fig. 2 showing the whirling motion at different location of the cutting edge-workpiece system. Fig. 3 shows both the Z and Y signals for the cutting edge-workpiece system. Fig. 4 is a one-figure plot of the system showing the whirling motion at different locations of the workpiece at $\bar{x} = 0.1$, $\bar{x} = 0.3$, $\bar{x} = 0.5$, $\bar{x} = 0.7$, and $\bar{x} = 0.9$. Table 4 shows Whirl Diameters for Fig. 2 at different locations on the workpiece. The maximum whirl diameter is in Fig. 2(c) at the cutting edge-workpiece interaction.

The whirling motion is oscillating around zero. This is due to the assumption of the force terms in the Y and Z direction.

$$
\begin{aligned}
F_{cy}(t) &= F_{c_o y} \cos(\omega t) \\
F_{cz}(t) &= F_{c_o z} \sin(\omega t)
\end{aligned} \tag{43}
$$

This excitation that produces the latter originates from within the complete system of the cutting edge-workpiece system and the nature of the drilling process.

3. Conclusions

A mathematical approach was developed to study the whirling motion of the lathe machine at the intermediate turning stage. This model has been used to simulate the whirling motion at

different locations of the cutting edge-workpiece system. The mathematical model to study the whirling motion of the cutting edge–workpiece assembly transformed the homogenous equations with nonhomogeneous boundary condition into a problem with nonhomogeneous equations with homogenous boundary conditions. The computed fundamental natural frequency of the cutting edge-workpiece system was 24 Hz. The whirl amplitude was the highest at $\bar{x} = 0.5$ and the lowest was at $\bar{x} = 0.1$.

Acknowledgments

The authors would like to thank the Research Center, College of Engineering, King Saud University for supporting this work. The assistance and encouragement of the Research Center are very much appreciated.

Appendix A

$$\int_0^t \mathrm{e}^{-\varsigma\omega(t-\tau)} \sin\omega(t-\tau)\,\mathrm{d}\tau = -\frac{1}{\omega(\varsigma^2+1)}(-1+\mathrm{e}^{-\varsigma\omega t}\cos(\omega t)+\mathrm{e}^{-\varsigma\omega t}\sin(\omega t))$$

$$\int_0^t \cos(\omega\tau)\,\mathrm{e}^{-\varsigma\omega(t-\tau)} \sin\omega(t-\tau)\,\mathrm{d}\tau = -\frac{1}{\omega\varsigma(\varsigma^2+4)}\begin{pmatrix} -2\sin(\omega t)-\varsigma\cos(\omega t) \\ +\varsigma^2\mathrm{e}^{-\varsigma\omega t}\sin(\omega t) \\ +2\mathrm{e}^{-\varsigma\omega t}\sin(\omega t)+\varsigma\mathrm{e}^{-\varsigma\omega t}\cos(\omega t)\end{pmatrix}$$

$$\int_0^t \sin(\omega\tau)\,\mathrm{e}^{-\varsigma\omega(t-\tau)} \sin\omega(t-\tau)\,\mathrm{d}\tau = \frac{1}{\omega\varsigma(\varsigma^2+4)}\begin{pmatrix} \varsigma\sin(\omega t)-2\cos(\omega t)+\varsigma\mathrm{e}^{-\varsigma\omega t}\sin(\omega t) \\ +2\varsigma\mathrm{e}^{-\varsigma\omega t}\cos(\omega t)\end{pmatrix}$$

References

Al-Wedyan, H., Bhat, R., Demirli, K., 2007. Whirling vibrations in BTA deep hole boring process, Part 1: analytical and experimental investigations. Transactions of the ASME, Journal of Manufacturing Science and Engineering 129, 48–62.

Al-Wedyan, H., Bhat, R., Demirli, K., 2010. Active control of whirling vibrations in BTA deep hole boring process using two electrodynamic shakers. Control and Intelligent Systems 38 (4), to appear.

Bingwei, S., Zhenyue, Ma., Hironori, H., 2010. Rotordynamic moment on the backshroud of a Francis turbine runner under whirling motion. Journal of Fluids Engineering 132, 9.

Fujii, H., Marui, E., Ema, S., 1986a. Whirling vibration in drilling. Part 1: cause of vibration and role of chisel edge. Transactions of ASME, Journal of Engineering for Industry 108, 157–162.

Fujii, H., Marui, E., Ema, S., 1986b. Whirling vibration in drilling. Part 2: influence of drill geometries, particularly of the drill flank, on the initiation of vibration. Transactions of ASME, Journal of Engineering for Industry 108, 163–1168.

Fujii, H., Marui, E., Ema, S., 1988. Whirling vibration in drilling. Part 3: vibration analysis in drilling workpiece with a pilot hole. Transactions of ASME, Journal of Engineering for Industry 110, 315–321.

Koak, K., Jang, G., Kim, H., 2009. Whirling, tilting and axial motions of a HDD spindle system due to the manufacturing errors of FDBs. In: Special issue on 17th ASME Conference on Information Storage and Processing Systems, Santa Clara, CA, USA, 18–19 June 2009, pp. 1701–1709.

Lee, S., Eman, K., Wu, S., 1987. An analysis of the drill wandering motion. Transactions of ASME, Journal of Engineering for Industry 109, 297–305.

Minis, I., Magrab, E., Pandelidis, I., 1990a. Improved methods for the prediction of chatter in turning, Part 1: determination of structural response parameters. Transactions of ASME, Journal of Engineering for Industry 112, 12–20.

Minis, I., Magrab, E., Pandelidis, I., 1990b. Improved methods for the prediction of chatter in turning, Part 2: determination of cutting process parameters. Journal of Engineering for Industry 112, 21–27.

Minis, I., Magrab, E., Pandelidis, I., 1990c. Improved methods for the prediction of chatter in turning, Part 3: a generalized linear theory. Transactions of ASME, Journal of Engineering for Industry 112, 28–35.

Rahman, M., Seah, k., Venkatesh, V., 1988. Performance evaluation of endrills. International Journal of Machine Tools and Manufacture 28, 341–349.

Roukema, J., Altintas, Y., 2007. Generalized modeling of drilling vibrations. Part I: time domain model of drilling kinematics, dynamics and hole formation. International Journal of Machine Tools & Manufacture 47, 176.